Structural Study of SrTiO3 Doped with Mn Using X-Ray Diffraction

Zainab Ibrahim Booq, Sara Khalid Alghaith
Science College of King Saud University, Department of Physics and Astronomy
Turky Alaual, Riyadh, middle, Saudi Arabia, 11451
Zbooq@ksu.edu.sa; S.al_ghaith@hotmail.com

Abstract – *Monocrystalline Mn:SrTiO$_3$ was prepared from the compounds MnO$_2$, TiO$_2$, and SrCO$_3$, which had equivalent weights of 2.52 g. Mn was doped in this sample at 60 mol%. The sample was heated half hour, and annealed at 1223 K (950 ℃). The sample had an orientation of (100). The study was performed at room temperature (T = 300 K = 27 ℃). The structure of this crystal was investigated using X-ray diffraction and found to be cubic (P m$\bar{3}$m). The lattice parameter of the Mn:SrTiO$_3$ crystal was 3.269 Å. The grain size of this crystal was magnified 5,000–100,000 times using scanning electron microscopy and found to be in range of 1.33µm–91.4nm.*

1. Introduction

Strontium titanate oxide (SrTiO$_3$ or STO) crystal is a perovskite oxide material (ABO$_3$, where A is the rare earth element, B is the titanate, and O$_3$ is the oxide) [1]. This group of materials has a wide range of applications, including uses in transistors, receivers, and non-vital memory devices [2]. It is a semiconductor material [3], but becomes a superconductor when doped with Mn or any other transition metal ion [4, 2, 5]. This characteristic is responsible for the development of numerous physical properties, including good conductivity and magnetic properties [4, 6].

It is worth mentioning that the preparation methods for most ABO$_3$ crystals are very similar. Several preparation techniques have been developed to produce Mn:SrTiO$_3$ nanoparticles, including a sol–gel method, organic precursor method [7], powder sample method [8], and solution method at high temperatures [4, 8, 9, 10].

In this study, a monocrystalline sample of Mn:SrTiO$_3$ was prepared using a solution method at a high temperature, where Mn was used to dope the SrTiO$_3$ crystal [4, 8, 9, 10]. Then, X-ray diffraction (XRD) was used to investigate the structure. This was the first study to investigate the structure of this crystal using a low-resolution XRD device with a maximum current intensity was I = 1 mA and voltage V = 25 kV. The grain size was determined using scanning electron microscopy (SEM). The crystal preparation was complicated because available literature is not sufficiently clear, and there are different methods for doping the crystal and annealing at high temperatures, which requires a special furnace. In addition, special skill is required to adapt the low-resolution XRD device.

2. Material and Methods
2.1. Preparation of Mn:SrTiO$_3$ Monocrystal

The Mn:SrTiO$_3$ monocrystal was prepared using powders of MnO$_2$, TiO$_2$, and SrCO$_3$ [4, 8, 9, 10] with purities of 70%, 99%, and 98%, respectively. These compounds were added by equal weights of 2.52. g of each of the compounds were used [8] , so that SrTiO$_3$ was heavily doped by Mn at 60 mol%. The powders were mixed under magnetic stirring for 1 h to obtain a homogenous mixture. Then, the mixture was soaked in

de-ionized (DI) water for 20–25 min [11, 12]. A 3:1 by volume HCL:HNO₃ acidic solution was added and mixed for 12 min [13, 12]. The sample was annealed by being heated in a furnace at atmospheric pressure and temperature up to 1223 K (950 °C) over a period of half hour, and then cold [11, 14, 4]. It was then ground and pressed [24, 15, 16] to form a pellet with a thickness of 3 mm and diameter of 12 mm. Thus, the monocrystal was formed. The surface of this pellet was purified using acetone [2]. The steps for preparing the monocrystal are shown in figure (1).

A   B   C

D   E
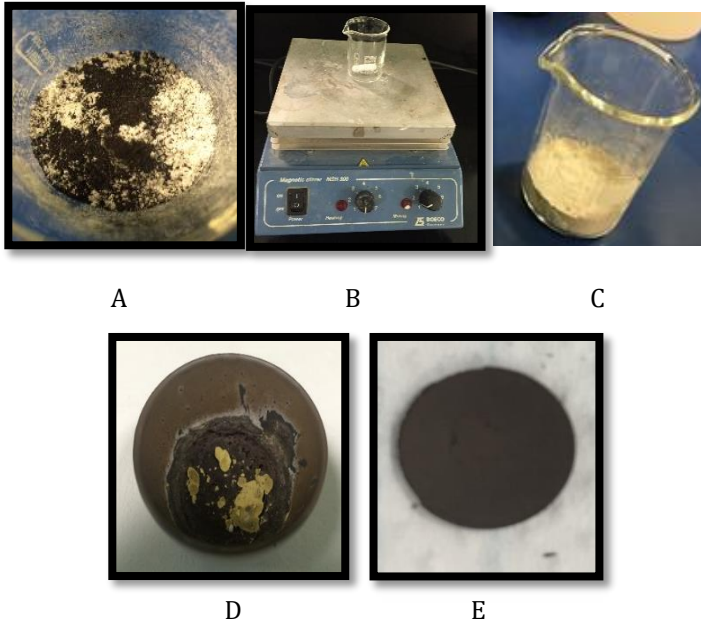
Figure 1. A. Powder compound mixing. B. Magnetic stirrer. C. Homogenous sample after stirring. D. Sample after annealing. E. Mn:SrTiO₃ monocrystal with thickness of 3 mm and diameter of 12 mm.

2.2. Study Methods

XRD was used to study the structure of this monocrystal by a low-resolution device (X-ray apparatus 55481) with a molybdenum anode, maximum current intensity I = 1 mA, and voltage V = 20 kV [17], as shown in fig (2, A). The monocrystal was polished using platinum materials, and then SEM (JSN-7610) was used to determine its grain size, as shown in figure (2, B).
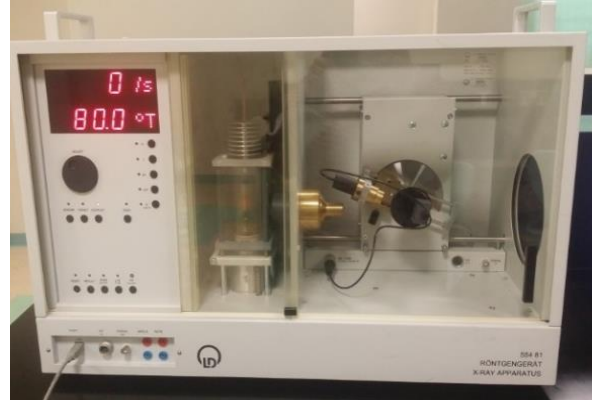
A

B

Figure 2. A. XRD (X-ray apparatus 55481) device. B. SEM (JSN-7610) device.

3. Results and Discussions
3.1. Structural Study using XRD

The best spectrum of this monocrystal was obtained in several steps. In the first step, the voltage was varied (V = 10, 15, 20, and 25 kV), while the current intensity was fixed at I = 1 mA, as shown in figure (2). From this figure, it is clear that at a high voltage, the deformation in the shape of the spectral lines is duplicated in some parts of the spectra more than in the others. This indicates a large electron emission from the cathode to the anode, which made it difficult to investigate the number of reflection planes. At a low voltage, it should be noted that the spectrum has a small number of lines. In other words, the number of reflection planes in the crystal decreased because there were several electrons in the cathode that could not gain enough energy to arrive at the anode. For this reason, the X-rays coming from the source were very weak, which made it difficult to see the full crystal [17]. As seen in figure (3), the best spectrum of this monocrystal was clearly found at a voltage V = 20 kV, and the number of

reflection planes (lines) agrees with the other results [9]. The sample was grown in the direction of the [100] plane, based on a calculation for the axial axis.
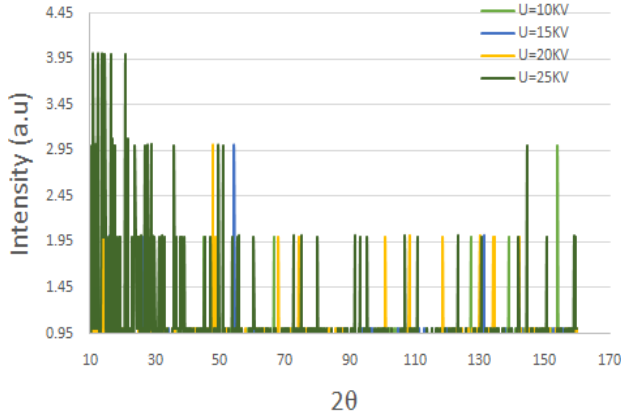
Figure 3. Spectrum lines of Mn : SrTiO₃ with variable voltage.

The second step involved varying the current intensity (I = 0.5, 0.7, 0.75, and 1 mA), while fixing the voltage V = 20 kV, as shown in figure (4). At a low current intensity, the number of reflection planes decreased because the number of electrons emitted from the cathode and arriving at the anode was low, which prevented all of the planes in the crystal from being seen. The best spectrum lines found in this step were at I = 1 mA, which agreed with the number of lines reported in the literature [15, 18].
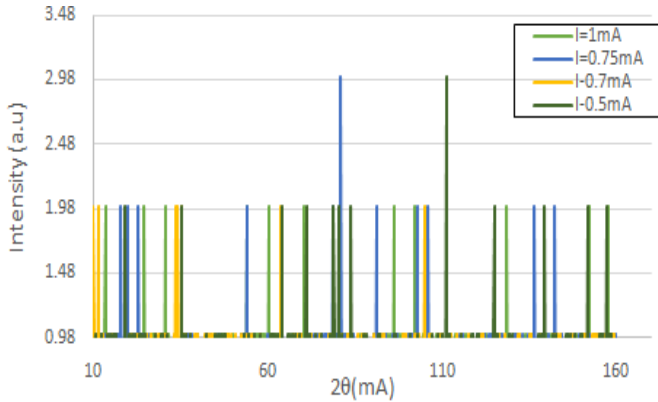
Figure 4. Spectrum lines of Mn:SrTiO₃ with variable current intensity.

Finally, the best spectrum was found for Mn:SrTiO₃ at a current intensity I = 1 mA, voltage V = 20 kV, and T = 300 K (27 ⁰C), as shown in figure (5). It consisted of eleven reflection planes, which agreed with the results of other studies [9, 18].
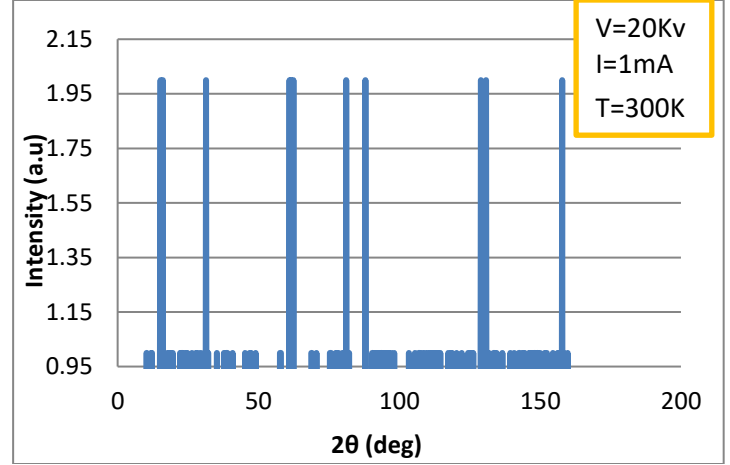
Figure 5. Best spectrum lines of Mn:SrTiO₃ crystal.

The X-ray wavelength of the best spectrum was calculated using equ. (1).

$$\lambda = \frac{hc}{eV} \tag{1}$$

$$\lambda = \frac{1.24 \times 10^{-6}}{V} \tag{2}$$

$$\lambda = 0.62 \dot{A} \tag{3}$$

Where λ is wavelength, h is plank constant, e is electron charge and V is voltage. The lattice parameter (a), which was approximately equal to the distance (d) between the planes in the crystal, was calculated from the slope in figure (6) and Bragg's law (equ. (4)), as shown in the following equations [19]:

$$n\lambda = 2d\sin\theta \tag{4}$$

$$a = \frac{slope}{2} \tag{5}$$

$$a = 3.269 \dot{A} \pm (0.008\%) \tag{6}$$

Where n the number of reflection planes, d is the distance between the reflection planes and a is the lattice parameter. The lattice constant value obtained from the experimental data was nearly the same as that found by others [8, 20, 9]. The reason for the very small differences between our lattice parameter result and that of others was the ratio of Mn doped in the STO, which was very high (heavily doped) in this study compared to others. If the doping in the crystal

increased, the value of the lattice parameter decreased and vice versa [20].
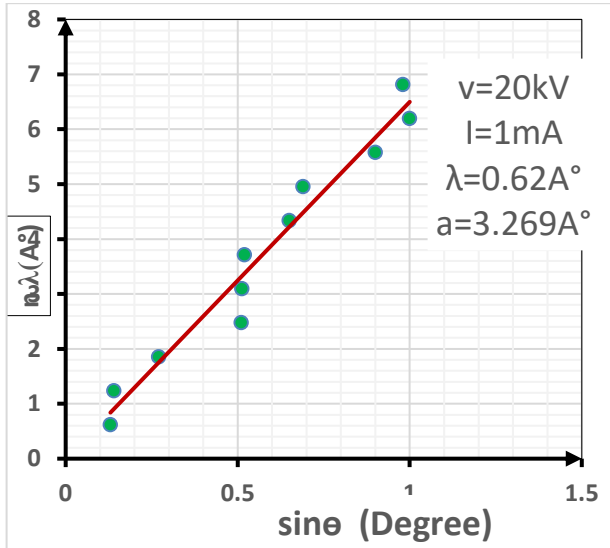
Figure 6. Relation between wavelength of reflection order (nλ) and diffraction angle (θ).

The crystal structure factor was calculated from the atomic scattering factor (f) and spectrum intensity (R), as shown in equation (7) and figure (7) [19].

$$R_{h,k,l} = |f_{h,k,l}^2|$$ (7)
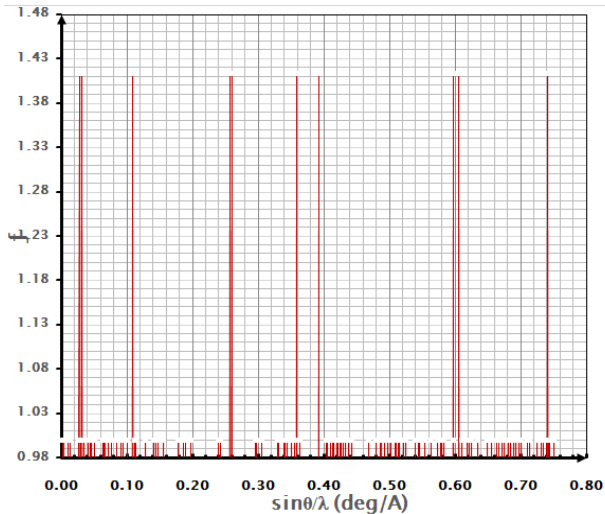
Figure 7. Relation between atomic scattering factor and (sin$\boldsymbol{\theta}$/λ).

In equation (7) R is peak intensity, h, k, and L are the Miller indices in the x, y, and z directions, respectively. The atomic scattering factor (F) is constant in figure (6). Thus, the crystal structure factor (S) can be calculated using equ. (8) and figure (6). The crystal

structure had a value equal to zero, as shown in equ. (10) [21].

$$S = \sum_n f_n e^{2\pi(hu+kv+lw)}$$ (8)

$$S = \frac{(f_1 - f_2)}{|f_1 - f_2|} + \Delta f$$ (9)

$$S = 0$$ (10)

Here, n is the number of atoms in the molecule; u, v, and w are the cut parts along the x, y, and z axes, respectively; and e is an exponential function. The structural factor was zero. Thus, this crystal was cubic, of type ($P\,m\bar{3}m$), as shown in figure (8) [21, 22]. This result agreed with those of others [2, 21, 22], where Mn^{2+} substituted for Sr^{2+} and Mn^{4+} substituted for Ti^{4+} [23,1, 10, 24].
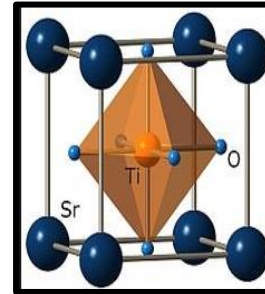
Figure 8. Structure of $Mn:SrTiO_3$ crystal ($P\,m\bar{3}m$) [25].

3.2. Calculating Grain Size using SEM Technique

There are several techniques for elemental analyses at a specific location using SEM and transmission electron microscopy (TEM). SEM is used to analyze the surface and obtain information about the particle size, and TEM is used to determine the internal structure of a solid [26].

The grain size of this monocrystal was calculated using SEM, as shown in figure (9), with a magnification of 5,000 times. The grain size of the crystal was in the range of 1.33–1.39 μm when magnified 5,000 times, but it was in the range of 84.9–91.4 nm when magnified 100,000 times. The grain size changed with the level of magnification [27]. This result agreed with those of others [7]. The grain size of the crystal depended on the doping ratio of the crystal. If the doping ratio of the crystal increased, the grain size decreased [20, 9]. Table (1) provides a brief summary of the results.

4
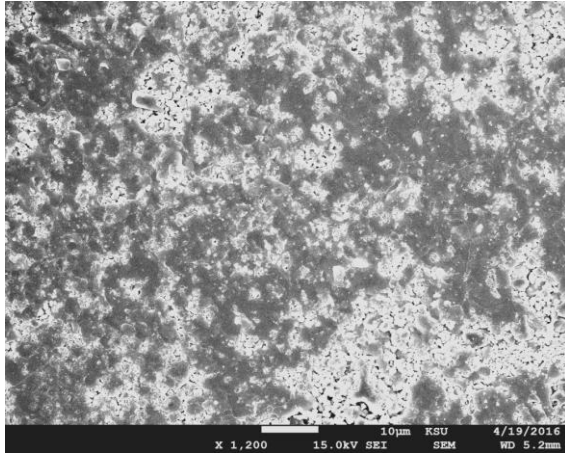
A
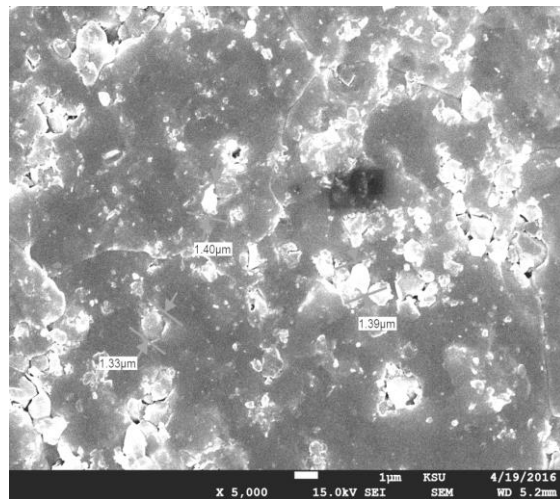
B
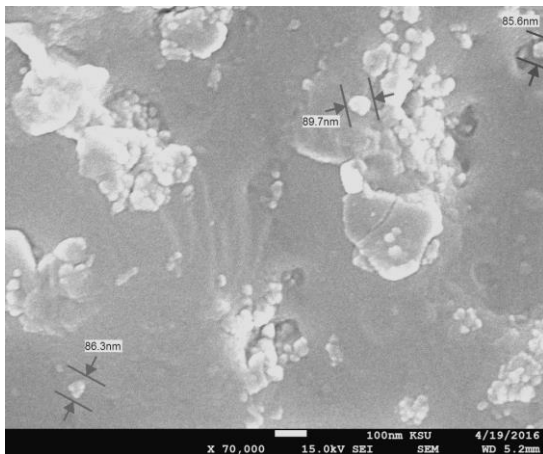
C
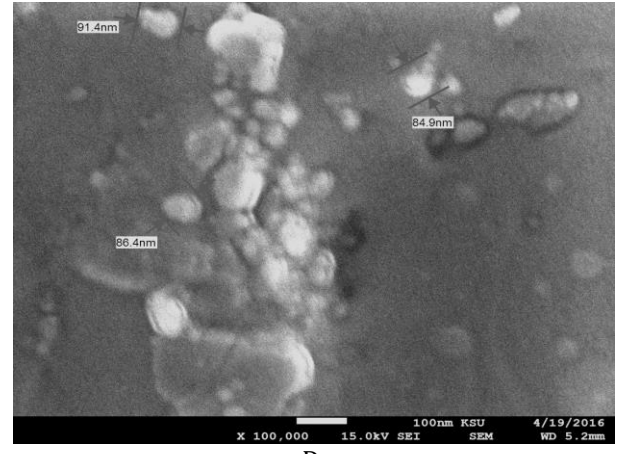
D

Figure 9. Mn : SrTiO$_3$ crystal at different magnifications (1,500–100,000), showing differences in grain size (1.33 µm to 91.4 nm).

Table 1. Brief summary of results.

Wavelength	λ = 0.62 Å
Mn ratio in crystal	60% mole percent
Sample size	thickness 3 mm diameter 12 mm
Annealing temperature	1223 K = 950 °C
Crystal temperature	300 K = 27 °C
Lattice parameter (a)	a = 3.269 Å
Crystal structure type	($P\,m\bar{3}m$) cubic
Crystal grain size	1.33 µm to 91.4 nm

4. Conclusion

This was the first structural study of Mn:SrTiO$_3$ with 60 mol% of Mn doped in the STO. It was investigated using a low-resolution XRD device, and the results obtained were the same as those of a neutron diffraction study of STO doped with Mn. The structure of this crystal was a cubic type ($P\,m\bar{3}m$) in the direction of the [100] plane, and the lattice constant was 3.269 Å. The grain size was in the range 1.39µm –91.4nm when magnified 5,000 to 100,000 times.

5. Acknowledgment

References

[1] F. M. F. De Groot, M. Grioni and et. al., "Strontium titanate," in *Properties of strontium titanate*, pp. 1-21, 2016.

[2] D. Choudhury, "Site-specific doping, tunable dielectric properties, and intrinsic paramagnetism in Mn-doped SrTiO3," *Pramana J. Phys.,* vol. 84, no. 6, pp. 987-997, 2015.

[3] M. D. Biegalski, D. D. Fong and e. al., "Critical thickness of high structural quality SrTiO3 films grown on orthorhombic (101) DySc03," *Journal of Applied Physics,* vol. 104, pp. 114109, 2008.

[4] T. Fix, F. Schoofs and et. al., "Influence of doping at the nanoscale at LaALO3:SrTiO3 interfaces," *Appl. Phys. lett.,* pp. 072110-1072110-3, 2010.

[5] L. P. Gor'kov, "Phonon mechanism in the most dilute superconductor: n type SrTiO3," in *PNAS*, Tallahassee, vol. 28, pp. 4646–4651, 2016.

[6] M. C. Gallardo, A. I. Becerro and et. al., "Cubic–tetragonal phase transition in $Ca_{0.04} Sr_{0.96} TiO_3$: A combined specific heat and neutron diffraction study," *J. Phy. Condens. Matter,* vol. 15, no. 2, pp. 91–100, 2002.

[7] R. M. Mohamed, M. M. Rashad and et. al., "Structure and magnetic properties of nanocrystalline cobalt ferrite powders synthesized using organic acid precursor method," *J. Magn. and Magn. Mat.,* vol. 322, no. 14, pp. 2058–2064, 2010.

[8] C. B. Azzoni, M. C. Mozzati and et. al., "Magnetic investigation of Mn ions in La,Mn:SrTiO," *Solid State Communications,* vol. 116, no. 6, pp. 303–308, 2000.

[9] D. Choudhury, R. M. Goodbole and et. al., "Top polarization, forward-backward asymmetry, and new physics," *Phys. Rev D.,* vol. 84, pp. 125–124, 2011.

[10] D. Choudhury, S. Mukherjee and et. al., "Tuning of dielectric properties and magnetism of SrTiO3 by site-specific doping of Mn," *A. B. Phys.,* vol. 53, pp. 5061–5069, 2005.

[11] J. Choi, C. B. Eom and et. al., "Growth mode transition from layer by layer to step flow during the growth of heteroepitaxial SrRuO3 on (001) SrTiO3," *Appl. Phys. Lett.,* vol. 79, no. 10, pp. 1449-1447, 2001.

[12] M. Kareev, S. Prosandeev and et. al., "Atomic control and characterization of surface defect states of TiO2 terminated SrTiO3 single crystals," *Appl. Phys. Lett.,* vol. 93, pp. 202-228, 2008.

[13] J. Zhang, D. Doutt and et. al, "Depth-resolved subsurface defects in chemically etched SrTiO3," *Appl. Phys. Lett.,* vol. 94, pp. 092904–092908, 2009.

[14] A. Abadpour, "A sequential Bayesian alternative to the classical parallel fuzzy clustering model," *Information Sciences,* vol. 318, pp. 28–47, 2015.

[15] A. M. Dehkordi, S. Bhattacharya and et. al., "New insights on the synthesis and electronic transport in bulk polycrystalline Pr-doped SrTiO−δ," *Journal of Applied Physics,* vol. 117, pp. 055102, 2015.

[16] M. S. J. Mashall and M. R. Castell, "Shape transitions of epitaxial islands during strained layer growth: Anatase TiO3(001) on SrTiO3(001)," *Physical Review Letters,* vol. 102, pp. 146-102, 2009.

[17] L. D. Gmbtt, "Instruction sheet 554 82," Hurth, 2001.

[18] A. El-Sayed, "Influence of zinc content on some properties of Ni–Zn ferrites*," Ceramics International,* vol. 28, 2002, pp. 363–367.

[19] H. Kooijman, "Interpretation of crystal struncture determinations," Bijvoet Center for Biomolecular Research, CH Utrecht, 2005.

[20] C. Azzoni, M. C. Mozzati and et. al, "Magnetic evidence of different environments of manganese ions in Mn-substituted strontium titanate," *Solid State Communications,* vol. 114, no. 12, pp. 617–622, 2000.

[21] M. Roessle, "Basic of x-ray scattering," EMBO course 2012, 2009.

[22] M. Huijben, A. Brinkman and et. al, "Structure-property relation of SrTiO3–LaAlO3 interfaces," *Advanced Materials,* vol. 21, no. 17, pp. 1665–1677, 2009.

[23] F. R. Silly, M. Castell and et.al., "Bimodal growth of Au on SrTiO3_001," *Physical Review Letters,* vol. 96, no. 8, pp. 1–4, 2006.

[24] A. Tkach, P. Vilarinho and e.al. "Structure–microstructure–dielectric tunability relationship in Mn-doped strontium titanate ceramics," *Acta Materialia,* vol. 53, no. 19, pp. 5061–5069, 2005.

[25] Postnova. (2016) *Centrifugal field-flow fractionation principle* [Online]. Available: http://www.postnova.com/centrifugal-fff.html?gclid=CMbNkZ6Tg88CFYUy0wodgoAMEg

[26] T. Leisegang, H. Stöcker, and et. al, "Switching Ti Valence in SrTiO3 by a dc Electric Field," *Phys. Rev. Lett.* vol. 102, pp. 087601, 2009.

[27]   Deft Solid Solutions. (2016). *Scanning & transmission electron microscopy.* [Online]. Available: https://www.solids-solutions.com/rd/particle-sizing-and-particle-size-analysis/scanning-transmission-electron-microscopy/